Structural Arrest in Dense Star-Polymer Solutions

G. Foffi,[1] F. Sciortino,[1] P. Tartaglia,[1] E. Zaccarelli,[1] F. Lo Verso,[2] L. Reatto,[2] K. A. Dawson,[3] and C. N. Likos[4]

[1]*Dipartimento di Fisica and INFM Center for Statistical Mechanics and Complexity, Università di Roma La Sapienza,
Piazzale Aldo Moro 2, I-00185 Rome, Italy*
[2]*Istituto Nazionale di Fisica della Materia and Dipartimento di Fisica, Università di Milano, Via Celoria 16, I-20133 Milano, Italy*
[3]*University College Dublin, Irish Center for Colloid Science and Biomaterials, Department of Chemistry,
Belfield, Dublin 4, Ireland*
[4]*Institut für Theoretische Physik II, Heinrich-Heine-Universität Düsseldorf, D-40225 Düsseldorf, Germany*
(Received 29 January 2003; published 9 June 2003)

The dynamics of star polymers is investigated via extensive molecular and Brownian dynamics simulations for a large range of functionality f and packing fraction η. The calculated isodiffusivity curves display both minima and maxima as a function of η and minima as a function of f. Simulation results are compared with theoretical predictions based on different approximations for the structure factor. In particular, the ideal glass transition line predicted by mode-coupling theory is shown to exactly track the isodiffusivity curves, offering a theoretical understanding for the observation of disordered arrested states in star-polymer solutions.

Star polymers play an important role in soft condensed matter systems, since they have been shown to interpolate between hard colloids with a strong repulsive core on one side and the soft flexible polymeric systems on the other [1]. Star polymers are constituted by a given number of polymeric arms, called functionality f, tied to a common center. As the functionality increases, the system becomes more similar to a hard sphere (HS) system, while lowering the functionality the interparticle potential becomes increasingly soft. Recently, many interesting properties of star polymers have been clarified on the basis of an effective interaction potential between star polymer centers [2]. In line with their hybrid polymer-hard colloid character, star polymers display no crystallization transition when the functionality f is low, $f \lesssim 34$. At higher functionalities, a freezing transition takes place at about the overlap concentration of the system, into a bcc solid for lower functionalities and into an fcc solid for higher functionalities [3]. The freezing is succeeded by either a reentrant melting transition to the fluid for intermediate functionalities, $34 \lesssim f \lesssim 54$, or by a cascade of structural phase transitions at higher values of f. The functionality-dependent bcc and fcc solids [4,5], as well as the reentrant melting transition [6], have been experimentally observed in solutions of starlike block copolymer micelles. Though the crystalline solids are the phases of thermodynamic equilibrium at such high concentrations, the experimental situation is often somewhat different. A variety of studies with star polymers or starlike systems of various functionalities has shown that it is quite difficult to nucleate a crystal. Especially at high functionalities, the solutions display a gelation transition, i.e., a dynamical arrest into an amorphous crowded state in which the characteristic relaxation time of the system becomes extremely long [7–12]. The onset of gelation, as

opposed to crystallization, is further enhanced by the presence of some polydispersity in the samples, which gets indeed more pronounced as functionality increases.

The purpose of this work is to analyze the dynamics of star polymers in athermal solvents theoretically, by employing a combination of methods. Using the star-star effective interaction potential, in which all microscopically fluctuating degrees of freedom are averaged out, we carry out detailed molecular dynamics (MD) and Brownian dynamics (BD) simulations to measure the diffusivity of the star-polymer fluids down to the homogeneous nucleation limit. Moreover, we carry out a mode-coupling theory (MCT) analysis [13] of the long-time limit of the correlation functions, which allows us to locate the nonergodicity (ideal glass) transition line of the system. We find that, on increasing the number density of polymer, the characteristic time of the system goes through a sequence of maxima and minima which we show to be related to the oscillatory behavior of the effective HS diameter [14]. We also find a strong correlation between the equilibrium phase diagrams of the system and the ideal glass line. The equilibrium reentrant melting transition is shown to have its counterpart in the reentrant melting of the disordered glass nested between two stable fluid phases. Finally, we discover a striking similarity in the shape of the isodiffusivity and MCT ideal glass curves, regardless of the detailed approximation employed in the calculation of the structure factor $S(q)$ and the type of dynamics (MD or BD). These findings strongly support the interpretation that the structural arrest of star polymers is a glass transition of "effective hard spheres" characterized by an η- and f-dependent HS diameter, despite the fact that the liquid structure and the variety and nature of the equilibrium phases themselves is very different from the HS case.

Standard MD and BD techniques have been employed in order to study the dynamic behavior of the star-polymer system [15]. MD and BD lead to identical predictions for the long-time dynamics of the system within the framework of the MCT [13,16]. Thus, though BD offers a more realistic description of the short-time diffusion of the particles, the long-time behavior which is the relevant behavior for the glass transition is the same in both. Hydrodynamic interactions are ignored and the analysis is based on the effective center-center interaction potential

$$\beta V(r) = \frac{5}{18} f^{3/2} \left[-\ln\left(\frac{r}{\sigma}\right) + \frac{1}{1 + \sqrt{f}/2} \right], \qquad r \le \sigma$$
$$= \frac{5}{18} f^{3/2} \frac{\sigma/r}{1 + \sqrt{f}/2} \exp\left[-\frac{\sqrt{f}(r - \sigma)}{2\sigma} \right], \quad r \ge \sigma,$$
(1)

where $\beta = 1/k_B T$ and r is the distance between the two centers. This potential is a combination of a logarithmic interaction at short distances, which gives the interaction its ultrasoft character and stems from the scaling analysis of Witten and Pincus [17], and a Yukawa form for the decay at long distances matched at a distance $r = \sigma$. The quantity $\beta V(r)$ depends solely on σ and f. The validity of this potential has been demonstrated via extensive comparisons both with small angle neutron scattering data [2,10] and with monomer-resolved simulations [18]. In this entropic interaction, f^{-1} plays the role of T in normal fluids.

In order to locate the line of structural arrest, the mean squared displacement averaged over all particles $\langle |\mathbf{r}_i(t) - \mathbf{r}_i(0)|^2 \rangle$, where $\mathbf{r}_i$ is the position of particle i, has been computed as a function of time t for several values of the two control parameters, the functionality f and the packing fraction $\eta = \pi \rho \sigma^3 / 6$, where ρ is the number density. The values of the self-diffusion coefficient D are calculated from the relation $6Dt = \langle |\mathbf{r}_i(t) - \mathbf{r}_i(0)|^2 \rangle$, valid for large t.

For the same system, the MCT equations [13] for modelling the structural arrest in supercooled liquid states have been solved; MCT furnishes a time evolution equation for the normalized density fluctuation correlator $\Phi(q, t)$ as a function of the momentum transfer q and t, which contains a term nonlinear in the correlator itself. Knowing $S(q)$ for the given interaction potential, the memory kernel entering in the nonlinear term of the MCT equation can be evaluated and the equation solved for various values of q. In particular, the nonergodicity transition leading to structural arrest is obtained by performing the limiting value of the density correlator $\lim_{t\to\infty} \Phi(q, t) = f(q)$. The nonergodicity factor $f(q)$ is the solution of the equation

$$\frac{f(q)}{1 - f(q)} = \mathcal{F}_q(f),$$
(2)

where the memory kernel is quadratic in the correlator

$$\mathcal{F}_q(f) = \frac{1}{2} \int \frac{d^3 k}{(2\pi)^3} \mathcal{V}(\mathbf{q}, \mathbf{k}) f(k) f(|\mathbf{q} - \mathbf{k}|).$$
(3)

The vertex functions $\mathcal{V}$, the coupling constants of the theory, are

$$\mathcal{V}(\mathbf{q}, \mathbf{k}) = \frac{\rho}{q^4} [\mathbf{q} \cdot (\mathbf{q} - \mathbf{k}) c(|\mathbf{q} - \mathbf{k}|)$$
$$+ \mathbf{q} \cdot \mathbf{k} c(k)]^2 S(q) S(k) S(|\mathbf{q} - \mathbf{k}|) \quad (4)$$

and depend only on the Fourier transform of the direct correlation function $c(q)$, or equivalently on $S(q)$. In the A_2 bifurcation scenario of MCT [13] the solutions of Eq. (2) jump from zero to a finite value at the ideal glass transition. The locus of the fluid-glass transition can be calculated varying the control parameters of the system, f and η.

$S(q)$ has been calculated for the potential of Eq. (1) using two different approximate closures for the Ornstein-Zernike equation. The first one is the self-consistent Rogers-Young (RY) closure [19], which satisfies the thermodynamic requirement that the isothermal compressibilities calculated either following the so-called fluctuation route or the virial route be identical to one another. The second approach is the modified hypernetted-chain approximation (MHNC) [20]. In the MHNC, one approximates the bridge function of the system [21] with that of an effective HS fluid. The optimum value of the diameter of this reference HS system is chosen in such a way to satisfy the Lado criterion [22]. Both the RY and the MHNC closures have been shown to yield results that compare extremely well with simulations [14,23].

The diffusion coefficient D for MD and BD are reported in Fig. 1, in the upper and middle panels, respectively, for a large set of f and η values [24]. In simple liquids, D decreases monotonically on increasing η. In the present system, D has a highly nonmonotonic behavior. At $f = 32$ a minimum around $\eta = 0.5$ is followed by a flat maximum up to $\eta = 1.5$. At larger f values ($f > 40$) a clear sequence of minima and maxima is observed. The MD and BD results show the same trend, and in supercooled states the D values become proportional. Such a proportionality supports the interpretation of the present results in term of MCT for supercooled liquids. Indeed, one of the basic predictions of the theory is the independence of the slow dynamics from the microscopic dynamics [13,16,25].

The η and f dependence of D can be rationalized by calculating the isodiffusivity curves [26], i.e., the locus of points in the (η, f) plane where D has a constant value. Such curves, for two different values of D, are shown in Fig. 2 together with the equilibrium fluid-crystal coexistence lines, as calculated in Ref. [3]. The isodiffusivity curves run parallel to the coexistence lines, suggesting that crystallization in this system is achieved at the same D value, independently from the underlying crystalline
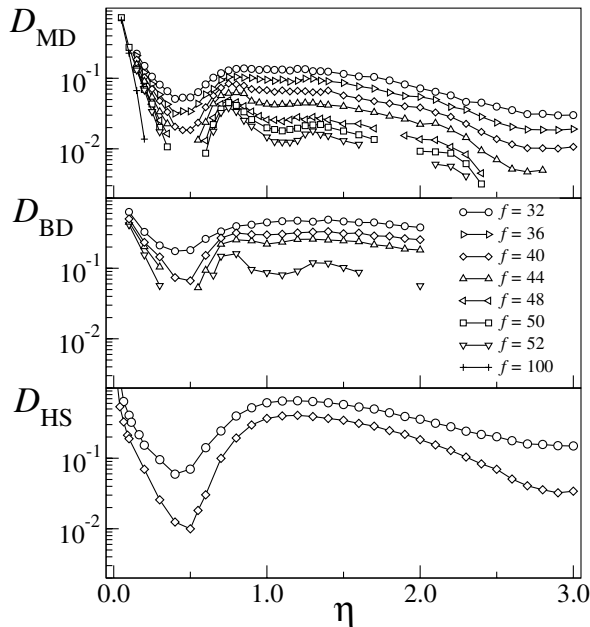
FIG. 1. The self-diffusion coefficient, D_{MD} obtained by molecular dynamics (upper panel, MD units [15]), D_{BD} by Brownian dynamics (middle panel, BD units), and D_{HS} for an equivalent HS system (lower panel, arbitrary units), as a function of packing fraction for various values of the functionality [24]. Missing points along the simulation curves were identified as crystalline states.

phase, and offering thereby a strong confirmation of the dynamical freezing criterion of Löwen *et al.* [27]. Figure 2 also shows the MCT ideal glass transition line (which can be considered as the isodiffusivity curve in the limit $D = 0$) using as input the RY and the MHNC $S(q)$. Both the RY and the MHNC ideal glass lines track the molecu-
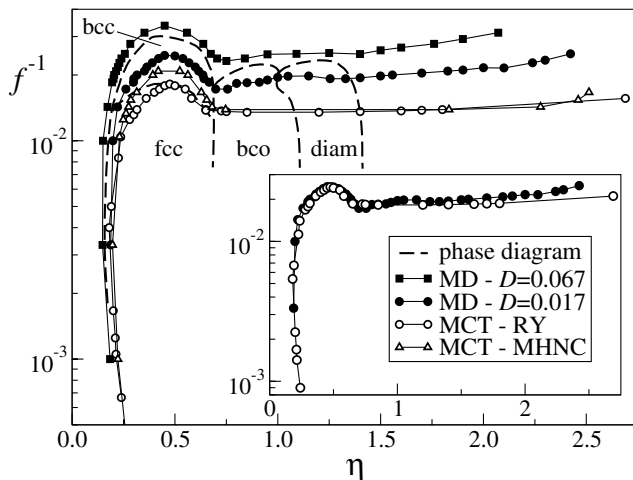

FIG. 2. Experimental isodiffusivity curves for two values of the MD-diffusion coefficient ($D = 0.067$ and $D = 0.017$) and the MCT fluid-glass lines (computed with RY and MHNC). The equilibrium phase diagram (from Ref. [3]) is also reported for comparison. The inset compares the RY-ideal MCT glass line with the isodiffusivity data for $D = 0.017$, after a shift along the f^{-1} axis.

lar dynamics isodiffusivity curves. The simulation curve can be perfectly superimposed to the theoretical curve after a shift in f^{-1}, as shown in the inset of Fig. 2. The agreement between theory and simulation below $\eta = 1$ is extremely good, independent of the f value. Even the reentrant shape of the isodiffusivity curve for $f > 500$ is captured by the theory.

The shape of the ideal glass line in the (η, f) plane suggests interesting possibilities for modulating the dynamics in star-polymer systems. If crystallization can be avoided, a glass state can be generated by compression which can then be melted with further compression (for example for $f = 36$). Similarly, the dynamics of the polymer can be slowed down and increased again upon increase of its functionality (for example at $\eta = 0.23$).

In order to better grasp the peculiar shape of the dynamical arrest curve, we test the hypothesis that the slowing down of the dynamics is controlled by the η and f dependence of an effective hard core. MHNC provides a well-defined way for calculating the equivalent HS diameter σ_{HS} and thus η_{HS}. In the case of the star-polymer potential, employing the Lado criterion [22] for the MHNC, the dependence of η_{HS} on η has already been studied and it has been shown that it reflects the features of the interparticle interaction [14]. On the other hand, values of the diffusion coefficient D_{HS} for HS systems as a function of η_{HS}, the HS packing fraction, can be easily obtained directly by MD simulation. In a similar way D_{HS} is known to follow for BD the simple law [28–30] $D_{HS} = D_0(1 - 2\eta_{HS})$ for $\eta_{HS} \leq 0.4$, with D_0 a constant. This offers the possibility of converting the known η dependence of the effective HS packing fraction, $\eta_{HS}(\eta)$, into an effective $D_{HS}(\eta)$ of the corresponding HS system (both for BD and MD). This, in turn, can be compared with the star-polymer D values reported here. The comparison for MD is shown in the lower panel of Fig. 1, which illustrates that the simple mapping between the packing fractions of the star-polymer η and the HS system η_{HS} captures the main features of the diffusion coefficient, e.g., the location of the minima and maxima of the curves. The agreement between the two sets of data suggests that the slow dynamics in star-polymer systems can be traced back—via a density- and functionality-dependent effective HS diameter—to the slow dynamics of the HS system (which is accurately described by MCT [31]).

Finally, Fig. 3 shows the nonergodicity factor $f(q)$ at three different representative points along the ideal glass line, calculated with the MHNC $S(q)$. The $f(q)$ shape changes continuously along the ideal glass line, going from the typical HS shape at small η (left-hand and central panel) to a much more structured shape at large η (right-hand panel). The $f(q)$ width is a measure of the inverse of the cage localization length, which decreases on increasing η. The q dependence of $f(q)$ is always in phase with $S(q)$, a feature common to all previously studied models. Two interesting features that develop at
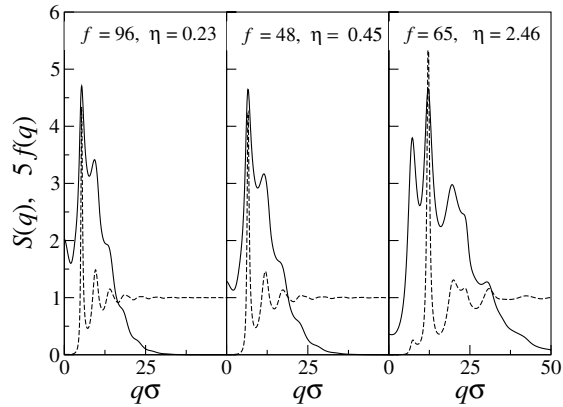
FIG. 3. The MHNC structure factor $S(q)$ (dashed line) and the nonergodicity factor $f(q)$ (solid line) for three representative points along the fluid-glass transition line.

large η are the significant increase in $f(q)$ in the q range at $q\sigma = 12.5$ and the small value for vanishing q.

The MD and BD simulation data reported in this Letter, for a large range of f and η, show that the dynamics of star-polymer solutions is extremely rich. The isodiffusivity curves have been shown to display both minima and maxima as a function of η and minima as a function of f which have been successfully connected to the behavior to the η- and f-dependence of the effective hard core diameter of an equivalent HS system, despite the significant differences between the star polymer and the HS $S(q)$. The detailed comparison between theoretical predictions and simulation confirms that MCT is a valid approach for guiding the interpretation of the disordered arrested states of soft matter materials [32,33], offering a theoretical understanding for the observation of disordered arrested states not only in colloidal systems characterized by a hard core [34–37] or charge-stabilized colloidal dispersions [38], but also in ultrasoft systems such as star-polymer solutions.

[1] C. N. Likos, Phys. Rep. **348**, 267 (2001), and references therein.
[2] C. N. Likos et al., Phys. Rev. Lett. **80**, 4450 (1998).
[3] M. Watzlawek et al., Phys. Rev. Lett. **82**, 5289 (1999).
[4] G. A. McConnell et al., Phys. Rev. Lett. **71**, 2102 (1993).
[5] G. A. McConnell and A. P. Gast, Phys. Rev. E **54**, 5447 (1996).
[6] G. A. McConnell and A. P. Gast, Macromolecules **30**, 435 (1997).
[7] D. Vlassopoulos et al., J. Phys. Condens. Matter **13**, R855 (2001).
[8] M. Kapnistos et al., Phys. Rev. Lett. **85**, 4072 (2000).
[9] B. Loppinet et al., Macromolecules **34**, 8216 (2001).
[10] J. Stellbrink et al., Progr. Colloid Polym. Sci. **115**, 88 (2000).
[11] E. Stiakakis et al., Phys. Rev. Lett. **89**, 208302 (2002).
[12] E. Stiakakis et al., Phys. Rev. E **66**, 051804 (2002).
[13] W. Götze, in *Liquids, Freezing and Glass Transition*, edited by J. P. Hansen, D. Levesque, and J. Zinn-Justin (North-Holland, Amsterdam, 1991), p. 287.
[14] F. Lo Verso et al., J. Phys. Condens. Matter **15**, 1505 (2003).
[15] The studied system is composed of 1000 particles of unitary mass m interacting via the potential of Eq. (1). Distances are measured in units of σ and time in units of $(m\sigma^2\beta)^{1/2}$, with $\beta = 1$. The integration time step is 0.005.
[16] G. Szamel and H. Löwen, Phys. Rev. A **44**, 8215 (1991).
[17] T. A. Witten and P. A. Pincus, Macromolecules **19**, 2509 (1986).
[18] A. Jusufi et al., Macromolecules **32**, 4470 (1999).
[19] F. A. Rogers and D. A. Young, Phys. Rev. A **30**, 999 (1984).
[20] Y. Rosenfeld and N. W. Ashcroft, Phys. Rev. A **20**, 1208 (1979).
[21] J. P. Hansen and I. R. McDonald, *Theory of Simple Liquids* (Academic, New York, 1986), 2nd ed.
[22] F. Lado, Phys. Lett. **89A**, 196 (1982).
[23] M. Watzlawek et al., J. Phys. Condens. Matter **10**, 8189 (1998).
[24] The studied (f, η) values correspond to states both in the equilibrium and in the supercooled region of the phase diagram. We report only state points where crystallization did not intervene within the time length of the simulation. Crystallization has been detected via the time evolution of the potential energy and of $S(q)$.
[25] For the case of supercooled binary Lennard-Jones, an accurate comparison between BD and MD has been reported in T. Gleim et al., Phys. Rev. Lett. **81**, 4404 (1998).
[26] G. Foffi et al., Phys. Rev. E **65**, 050802 (2002); E. Zaccarelli et al., Phys. Rev. E **66**, 041402 (2002).
[27] H. Löwen et al., Phys. Rev. Lett. **70**, 1557 (1993).
[28] P. Pusey, in *Liquids, Freezing and Glass Transition*, edited by J. P. Hansen, D. Levesque, and J. Zinn-Justin (North-Holland, Amsterdam, 1991).
[29] H. Löwen and G. Szamel, J. Phys. Condens. Matter **5**, 2295 (1993).
[30] B. Cichocki and K. Hinsen, Physica (Amsterdam) **166A**, 473 (1990).
[31] W. Götze, J. Phys. Condens. Matter **11**, A1 (1999).
[32] F. Sciortino, Nature Materials **1**, 145 (2002).
[33] K. A. Dawson, Curr. Opin. Colloid Interface Sci. **7**, 218 (2002).
[34] L. Fabbian et al., Phys. Rev. E **59**, R1347 (1999); **60**, 2430 (1999).
[35] K. A. Dawson et al., Phys. Rev. E **63**, 11401 (2000).
[36] K. N. Pham et al., Science **296**, 104 (2002).
[37] T. Eckert and E. Bartsch, Phys. Rev. Lett. **89**, 125701 (2002).
[38] S. K. Lai et al., Phys. Rev. E **56**, 766 (1997); S. K. Lai and G. F. Wang, Phys. Rev. E **58**, 3072 (1998); S. K. Lai et al., J. Chem. Phys. **110**, 7433 (1999); G. F. Wang and S. K. Lai, Phys. Rev. Lett. **82**, 3645 (1999).